Permeability of textile reinforcements: Simulation, influence of shear and validation

B. Verleye [a,*], R. Croce [b], M. Griebel [b], M. Klitz [b], S.V. Lomov [c], G. Morren [d], H. Sol [d], I. Verpoest [c], D. Roose [a]

[a] K.U.Leuven, Department of Computer Science, Celestijnenlaan 200A, B-3001 Leuven, Belgium
[b] University Bonn, Institute for Numerical Simulation, Germany
[c] K.U.Leuven, Department of Metallurgy and Materials Engineering, Belgium
[d] Vrije University of Brussel, Department of Mechanics of Materials and Constructions, Belgium

A B S T R A C T

The permeability of textile reinforcements is a crucial input for the simulation of the impregnation stage of a composite material fabrication process. In this paper, we present a fast and accurate simulation method for the permeability of a textile reinforcement, based on a finite difference discretisation of the Stokes equations. Results for single layer, multi-layer and sheared models are discussed. The influence of intra-yarn flow and periodic or wall boundary conditions are considered. We compare the numerically computed permeability values with experimental data.

© 2008 Elsevier Ltd. All rights reserved.

1. Introduction

The design of a mould for the production of composite parts is still a trial- and error process, or based on accumulated experience. This is however, expensive and waste producing. More and more, the mould filling stage of the resin transfer moulding process is simulated with software tools like PAM-RTM [1] or LIMS [2]. These tools require the input of the permeability of the textile reinforcement, not only for the straight textile, but also for the draped textile which is sheared locally.

Analytical formulas for the computation of the permeability of porous media such as textiles have been presented by several authors (Table 1). A drawback of analytical formulas, like the ones from Gebart [3], Berdichevski [4] and Phelan [5] is that they are only valid for simplified textile models. Still, these formulas are applied for validation of simulation software and for the computation of the intra-yarn permeability [6]. The permeability can also be determined by numerical simulation of the fluid flow through a textile model and the subsequent use of Darcy's law. In order to have a fast permeability predicting method, Long et al. reduce the 3D fluid problem to a simplified 2D model [7]. This Grid average approach is well suited for parametric studies, however, it is not clear for which type of textile structures the method gives sufficiently accurate predictions of the permeability [8]. Accurate predictions can be obtained by solving the 3D Navier–Stokes or Stokes

equations or by solving an equivalent lattice Boltzmann model. Simulation tools based on a lattice Boltzmann model use a regular grid and avoid the difficult mesh generation. However, in order to be useful for parametric studies, the calculation of the permeability must be accurate and fast, which is not the case with the available lattice Boltzmann software [9]. Direct solution of the Navier–Stokes or Stokes equations can be done by a finite element (FE) or finite difference (FD) approach. FE simulation tools which work on a non-structured mesh have the advantage that the geometry can be meshed accurately, but the disadvantage that they are not suited for automatic permeability computations since these solvers require the mesh generation of the fluid region between the yarns of the textile. Authors do not mention problems in that regard, however, we are not aware of publications with results for realistic volume fractions, where the textile model has sharper edges and thus for which the generation of an appropriate mesh is difficult [10–12].

We employ a three-dimensional FD solver: it works on a regular grid but more acceleration techniques for the resulting partial differential system of equations are available than for the lattice Boltzmann method. For the creation of the textile model, we use the WiseTex software [15–17]. WiseTex implements a generalised description of the internal structure of textile reinforcements on the unit cell level. The WiseTex models are the input for our permeability predicting software FlowTex.

In this paper, we present a mathematical model to predict the permeability and the numerical methods to solve the resulting equations. We validate the results of the simulations with experi-

---

* Corresponding author. Tel.: +32 16 327835; fax: +32 16 327996.
E-mail address: bart.verleye@cs.kuleuven.be (B. Verleye).

Table 1
Several methods for the prediction of the permeability of textiles

Method	Reference	Comment
Theoretical formulas	[3–5]	Inaccurate for realistic textiles
FE modelling	[10–12]	Cumbersome meshing
Lattice Boltzmann modelling	[9]	No acceleration techniques available
Grid2D	[7]	No validation for different kinds of textile
Pore network model	[13]	No satisfactory validation
Random walk methods	[14]	No satisfactory validation

mental data for non-crimp fabrics, for a plain woven fabric, a mono-filament fabric and a random mat is discussed. We show that our method gives accurate results for several classes of reinforcements. Additionally, we discuss the influence on the permeability of shear, of the domain boundary conditions and of the nesting of different layers.

2. Mathematical model

The permeability tensor $\mathbf{K}$ is a geometric characteristic related to the structural features of the textile at several length scales. For a porous medium, the permeability tensor is defined by Darcy's law

$$\langle \mathbf{u} \rangle = -Re\mathbf{K}\langle \nabla p \rangle. \tag{1}$$

with $\mathbf{u} = \mathbf{u}(x, y, z)$ the fluid velocity, Re the Reynolds number, $p = p(x, y, z)$ the pressure and $\langle \rangle$ denotes volume averaging.

In case of a creeping, single-phase, isothermal, unidirectional saturated flow of a Newtonian fluid, the inter-yarn flow is described by the incompressible Navier–Stokes equations

$$\begin{cases} \frac{\partial \mathbf{u}}{\partial t} + (\mathbf{u} \cdot \nabla)\mathbf{u} = -\nabla p + \frac{1}{Re}\Delta \mathbf{u} \\ \nabla \cdot \mathbf{u} = 0 \\ \mathbf{u}|_{\mathbf{n}} = 0 \quad \text{and} \quad \nabla p|_{\mathbf{n}} = 0 \text{ on } \gamma. \end{cases} \tag{2}$$

Here γ denotes the boundary of the fluid and the solid region and $\mathbf{n}$ is the outward-pointing unit normal vector on γ. The first equation states the conservation of momentum, the second equation states the conservation of mass.

For the Reynolds numbers we are dealing with, i.e. $Re \leqslant 1$, the non-linear convection term can be neglected. Since we are only interested in the steady state solution, the time derivative can be omitted. This results in the steady state incompressible Stokes equations

$$\begin{cases} \Delta \mathbf{u} - Re\nabla p = 0 \\ \nabla \cdot \mathbf{u} = 0 \\ \mathbf{u}|_{\mathbf{n}} = 0 \quad \text{and} \quad \nabla p|_{\mathbf{n}} = \frac{1}{Re}\Delta \mathbf{u}|_{\mathbf{n}} \text{ on } \gamma. \end{cases} \tag{3}$$

Note that for low Reynolds numbers the approximation $\nabla p|_{\mathbf{n}} = 0$ on the boundary is not valid, and that the momentum equation must be projected on the boundary [18]. To determine the permeability from (1), the solution of (2) or (3) must be computed. Homogenisation of the Stokes equations can be applied within the periodic domain of a textile and yields Darcy's law (1) on the macro-level (Fig. 1). In [19] we show that solving Eq. (2) or (3) to simulate the fluid flow and then using Darcy's law to compute the permeability, results in the same numerical value as using the definition of $\mathbf{K}$ arising from homogenisation theory.

Intra-yarn flow depends on the local permeability tensor of the yarn $\mathbf{K}_{\text{yarn}}$, and is described by the Brinkman equations [20]

$$\begin{cases} \Delta \mathbf{u} - Re\nabla p = \mathbf{K}_{\text{yarn}}^{-1}\mathbf{u} \\ \nabla \cdot \mathbf{u} = 0. \end{cases} \tag{4}$$

The Brinkman equations can be seen as an extension of Darcy's law and as a practical way to deal with the coupled problem of flow in a porous medium and flow in the free fluid domain. Angot [21] proved that the Brinkman model can be used for such situations with no explicit interface conditions. Thus, in (4) the additional term $\mathbf{K}_{\text{yarn}}^{-1}\mathbf{u}$ can be seen as a penalisation of (3). Eq. (4) converges to (3) for large $\|\mathbf{K}_{\text{yarn}}\|$. To compute the local permeability tensor $\mathbf{K}_{\text{yarn}}$, the fibres of the yarns are locally approximated as a regular array of cylinders. The components of $\mathbf{K}_{\text{yarn}}$ can then be computed according to the analytical formulas of Gebart [3] and Berdichevski [4].

3. Numerical approach

For flow simulations in the irregular geometry of a textile, we solve the Navier–Stokes equations (2) and the Stokes equations (3) numerically on a regular grid with a finite difference discretisation. To this end, the geometry of the yarns is approximated to first order. An example of a textile geometry and its first order approximation is shown in Fig. 2. In this section, we discuss some aspects of the solution technique of the equations. The complete numerical procedure is summarised in Fig. 3.

3.1. Boundary conditions

A boundary condition must be imposed between the yarn and the fluid region. If we neglect the intra-yarn flow, the yarns are treated as impermeable. Each grid point is then either located in the fluid domain ('fluid points') or in the solid yarn domain ('solid points'). At the boundaries between the fluid and the solid, no-slip boundary conditions are imposed. We use a second order discretisation of the PDEs except at the boundaries, where we use a first order discretisation. Since the geometry is approximated to first order, we cannot expect second order accuracy near the boundaries.
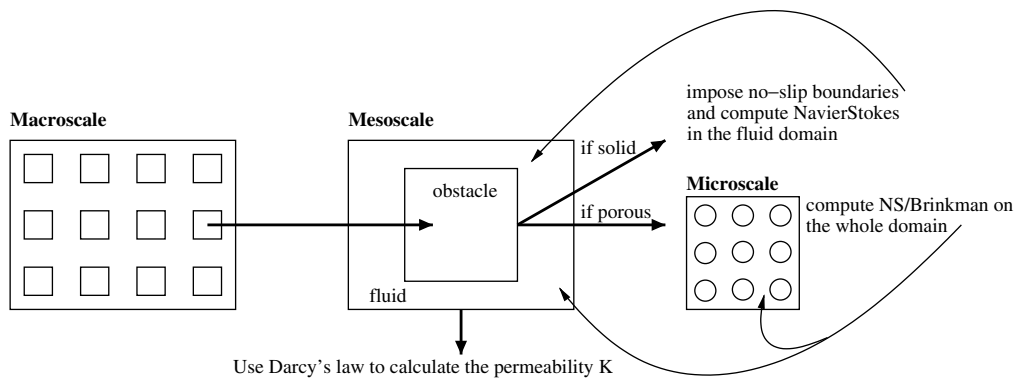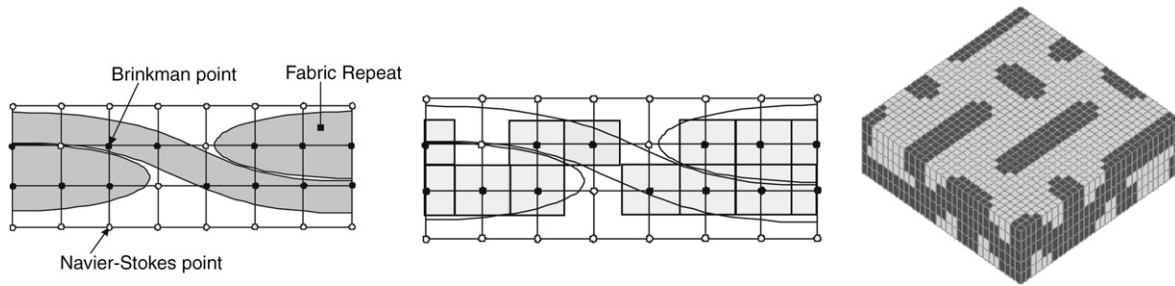

Fig. 1. The different scales and mathematical equations.

Fig. 2. A 2D-textile model (left) and its first order approximation on the grid (middle); 3D voxel geometry(right).
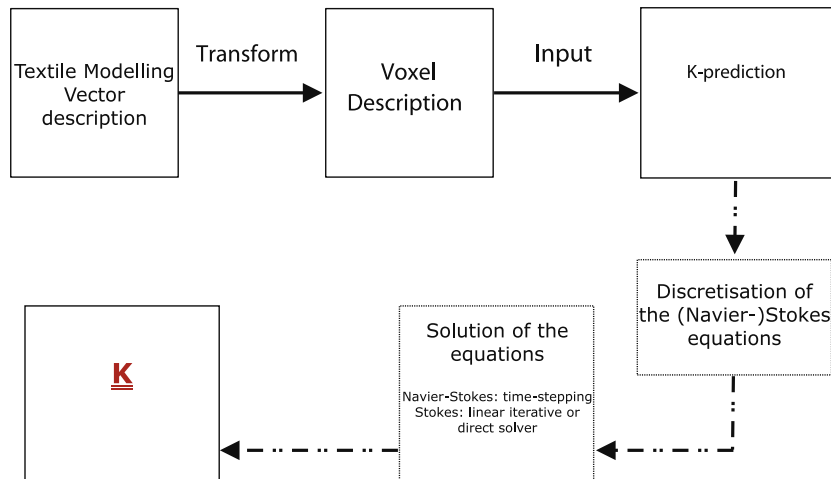

Fig. 3. Flowchart of the numerical procedure.

Including a second order description of the geometry would not only lead to the geometry modelling problems, but a second order approximation of the boundary would also impose additional numerical stability problems. Although using a first order approximation of the yarns means that fine meshes are required to obtain an accurate result, it is shown in the validation section that we obtain permeability values within an acceptable computation time (Section 5).

Boundary conditions must also be imposed on the boundary of the unit cell. In the X- and Y-direction (in-plane directions) it is obvious to use periodic boundary conditions because of the periodic structure of the textile. In the Z-direction (through the thickness direction) however, both periodic and wall conditions can be justified: several layers of textile are put on top of each other in the mould, so periodic boundary conditions are acceptable. However, the mould is closed under pressure, and the thickness of the textile specimen may be too small to neglect the influence of the closed mould. Moreover, if several layers are put inside a mould, nesting of the layers is inevitable. If two layers nest, they form a layer through which no fluid can flow in the Z-direction. In the validation section of this paper, we show a comparison of the possible boundary conditions with experimental results.

3.2. Solution of the Brinkman equations

The Brinkman equations (4) are similar to (3), and the same discretisation methods are used. They have to be solved in the yarn points if we take intra-yarn flow into account. We solve the Brinkman equations on the whole domain with $\|\mathbf{K}_{yarn}\| = \infty$ at fluid points (i.e. the Stokes equations), while $\|\mathbf{K}_{yarn}\|$ in the yarns is typically $10^{-4} \leqslant \|\mathbf{K}_{yarn}\| \leqslant 10^{-7}$.

3.3. Implementation

A finite difference Navier–Stokes solver, NaSt3DGP, was developed at the Institute for Numerical Simulation at the University of Bonn [22,23]. The flow solver employs a Chorin projection method on a staggered grid for the solution of the Navier–Stokes equations (2). In the staggered grid approach, the pressure is discretised at the centre of the cells, while the velocities are discretised on the side surfaces. This discretisation leads to a strong coupling between pressure and velocities, and therefore avoids the occurrence of unphysical oscillations in the pressure. From a numerical point of view, boundary conditions between the fluid and the solid region can be implemented in two ways:

- boundary values are set explicitly in the solid cells which are bordered by fluid cells;
- the boundary conditions are included in the equation to be solved in the boundary points in the fluid region.

NaSt3DGP sets the boundary values explicitly. On a staggered grid, this leads to the requirement that a solid point may not be bordered at two opposite sides by fluid points. When the solid region forms very fine structures, as is the case for random fibre assemblies, e.g. non-wovens, this constraint leads to a very fine mesh (finer than required to capture the geometry itself and to obtain a sufficiently accurate solution). More implementation details are discussed in [19].

The extension of NaSt3DGP towards a finite difference Stokes solver additionally uses the PETSc library [24] to solve the resulting system of discretised equations. Here, the discretisation has been realised on a collocated grid, i.e. all the unknowns are discretised in the centre of the cell, and includes the boundary conditions into

the discrete system matrix. Discretisation of the Stokes system (3) yields a saddle-point problem which can be written as

$$\begin{bmatrix} \Delta & \nabla^{\mathrm{T}} \\ \nabla & 0 \end{bmatrix} \begin{bmatrix} U \\ P \end{bmatrix} \approx \begin{bmatrix} A & B^{\mathrm{T}} \\ B & C \end{bmatrix} \begin{bmatrix} U \\ P \end{bmatrix} = \begin{bmatrix} f \\ 0 \end{bmatrix}, \qquad (5)$$

with A the diffusion matrix, B the mass conservation matrix, C equals 0 or contains stabilisation coefficients and f represents the external force on the system. System (5) is a linear system, and the PETSc library provides several iterative and direct methods to solve the equations. The generalised minimal residual method (GMRES) with an incomplete LU (ILU) preconditioner was used for the numerical experiments in this paper. Solving system (5) with $C = 0$ results in slow convergence to an unstable solution for P. Therefore, stability coefficients are added to the matrix C. Stabilisation terms of the form $\alpha h^2 \Delta p$ are added to the conservation equation, with α a free parameter and h the discretisation step in the respective direction [25,26]. The choice of α is not without consequences: a large α introduces an error in the continuity equation and results in a non-divergence free flow field. On the other hand, a small α results in slow convergence rate of the iterative solvers and if chosen too small, the stabilisation effect disappears and unwanted pressure oscillations are present in the solution. Our numerical simulations and experience lead to the appropriate choice of $\alpha = O(10^{-2})$.

4. Experimental set-up

The experimental prediction of the permeability on the majority of the textiles presented, is performed with a highly automated central injection rig, called PIERS set-up. This PIERS (permeability identification using electrical resistance sensors) set-up consists of a mould cavity with two sensor plates, each containing 60 electrical sensors. After placing the reinforcement and closing the mould, the test fluid can be injected. This is done centrally in the reinforcement through a hole in the middle of the lower sensor plate. While the flow front propagates through the reinforcement, the fluid flow makes contact with the electrical sensors. Since an electrical conductive fluid is used, the wetting of these DC-resistance sensors will change their electrical resistance. This variation is registered and hence an arrival time for the sensors can be stored. From this data, the experimentally determined permeability is computed with an inverse method [27–30].

5. Validation

In this section, our numerical predictions of the permeability are validated against experimental results. Experimental verification of computational methods for the simulation of textile permeability is often missing in the literature. We demonstrate that our method is a general approach, valid for several types of textile structures. This is an important difference to other permeability predicting methods which rely on the structure of the textile. For example, special methods for the prediction of the permeability of non-crimp fabrics are presented in [31].

5.1. Textile modelling

The methods and techniques to model woven textiles and non-crimp fabrics are explained in [15–17]. The multi-layered models, with or without nesting, are presented in [32].

The geometrical description of the internal structure of non-woven material is based on the following data:

- fibre volume fraction of the material;
- fibre geometrical (diameter, linear density) and mechanical properties;

- distribution of the fibre length;
- fibre orientation distribution (in- and out-of-plane), given as second order orientation tensor;
- fibre waviness, expressed as random combination of two harmonics.

The geometrical model uses these parameters of the individual fibres and creates a random fibrous assembly via a hierarchy of modelled objects:

- straight fibre, characterised by fibre properties, length and orientation;
- curved fibre, consisting of several straight intervals, and characterised by fibre properties, total length, averaged orientation of the intervals and shape of the fibre, generated using the given waviness parameters;
- random realisation of an assembly of a given number of (curved or straight) fibres. The boundaries of the unit cell of the material (where all the centres of gravity of the fibres are randomly placed) are calculated based on the given fibre volume fraction and thickness of the non-woven fabric. The number of fibres is randomly generated by the model according to the given distributions of length, orientation and waviness of the fibres. In the case of non-woven fabric (as opposed to bulk material) the orientation is corrected to fit all the fibres inside the given thickness of the fabric. The random realisation of a non-woven assembly is considered to be periodic; the degree of stochasticity included in the description is regulated by the number of the fibres in the assembly.

5.2. Experimental validation

Table 2 presents experimental and numerical results for two non-crimp fabrics, a bi-axial and a quadri-axial fabric, together with details of the computational parameters and the fabric data. The textile models are shown in Figs. 6–9. On the bi-axial structure, three institutes performed the experiments: MTM (K.U.Leuven), EPFL (Lausanne) and Ecole des Mines (Douai), and the presented experimental value is the result of an interpolation of the experimental values for different volume fractions. The non-crimp fabric has a dense structure which results in a high influence of the intra-yarn flow. For the quadri-axial non-crimp fabric the computed permeability without Brinkman flow is $5.3\,\mathrm{E} - 04\ \mathrm{mm}^2$, which would be a large underestimation of the experimental permeability.

The experimental permeability value is higher than the numerical value. To find the reason for this discrepancy, the influence of the stitching pattern and the size of the openings on the permeability is investigated in Table 3 for the Quadri-axial fabric. The stitching pattern has almost no influence on the permeability. On

Table 2
Details of the non-crimp fabrics

Parameter	Bi-axial	Quadri-axial
Number of plies	2	4
Orientation of plies (°)	+45; −45	0; −45; 90; −45
Mass of the fabric (g/m²)	322 ± 16	629 ± 31
Stitching pattern	Tricot	Tricot-chain
V_{f} (%)	38.5	41.2
Periodic b.c. in	XYZ	XYZ
K_{xx} Numerical (mm²)	5.0 E−4	8.8 E−4
K_{xx} Experimental (mm²)	1.3 E−3	2.1 E−3

Table 3
Influence of the opening size on the permeability of non-crimp fabrics

Parameter	Q orig	Q1	Q2	Q3
Stitching pattern	Tricot-chain	Tricot	Tricot-chain	Tricot-chain
V_f (%)	41.2	41.2	41.2	41.2
Opening size (mm)	0.66/0.18	0.66/0.18	0.62/0.18	0.71/0.08
	0.18/0.48	0.18/0.48	0.18/0.44	0.18/0.53
K_{xx} Num. (mm²)	8.8 E−4	8.8 E−4	8.1 E−4	9.6 E−4

The four values for the opening size relate to the four plies.

Table 4
Details of the woven fabrics geometries

Parameter	PWF	MFF	Random mat
Width warp yarns (mm)	2.21	0.75	NA
Gap warp (mm)	0.58	0.44	NA
Width fill yarns (mm)	2.79	0.66	NA
Gap fill (mm)	0.35	0.34	NA
Areal density (g/m²)	420	390	580
Specific density (kg/m³)	2520	1423	2520
Yarn tex warp (g/km)	580	115	NA
Yarn tex weft (g/km)	600	115	NA
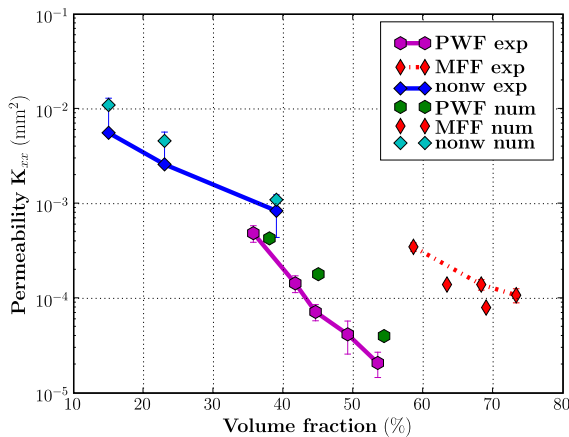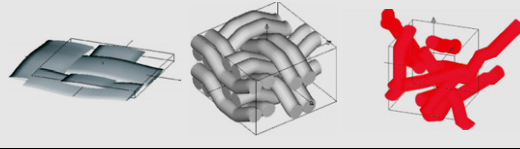
Fig. 4. Experimental and numerical data of the PWF, MFF and the random mat.

the contrary, a small change in the size of the openings has a significant effect on the permeability value. So probably the size of the openings of the non-crimp fabrics was slightly underestimated, which results in an underestimation of the permeability.

Table 4 presents for two woven fabrics a picture of the textile model and the parameter details. The computed permeabilities of the mono-filament fabric (MFF) and the plain woven fabric (PWF) are depicted in Fig. 4. For both textiles results with different volume fraction V_f are presented. For the low values of V_f, the computation was performed on a single layer model with wall boundary conditions. Although the experiments are performed on several layers, periodic boundary conditions yield an overestimation of the permeability as the layers will nest and form a wall around the other layers. Note that, in case of a non-crimp fabric we used peri-

odic boundary conditions since nesting does not occur in that case. The high V_f result is obtained by modelling a three layered model with maximal nesting. Then, the middle part of the model, where the nesting actually occurs, is extruded, and wall conditions are imposed.

Fig. 4 also presents the results for a non-woven random mat. Unfortunately for this random structure no detailed information is available (Table 4). However, given a certain V_f and a diameter of the fibres taken from the available picture, the geometry is approximated as well as possible (Fig. 10), and the computed permeability values are close to the experimentally obtained values. The computed value is an average of computations on five random structures.

We applied our permeability computing method for the computation of the permeability of various textile models. The software was used to compute the permeability of woven fabrics, non-crimp fabrics and non-woven fabrics. For all these materials, the computed results are compared with experimentally obtained permeability values. For the non-woven fabric, the numerical permeability values lie inside the error-bars of the experimental predictions. For the woven fabrics, a relative difference of 40–50% between the experimental and numerical values is observed. The numerical results are better for the lower volume fractions. This is what could be expected: the model of the low volume fraction is based on measurements on the textile layers of the final composite part. For the higher volume fractions, however, deformations like nesting and compression had to be modelled and some improvement on the modelling of high volume fraction textile models is possible. Nevertheless, our results present an important contribution compared to publications on other permeability simulation tools, for which often experimental validation lacks or results for higher volume fractions are not reported. Moreover, several of the latter simulation tools are only applicable to one specific type of textile (Table 1), or have empirical parameters.

5.3. Influence of shear

WiseTex allows the modelling of shear on the textile [33]. However, the sheared unit cell has no orthogonal repeat. This means that the periodic boundary conditions of the simulation software have to be put parallel to the direction of shear, and not, like in the original case, parallel to the orthogonal system axis. We have adapted our simulation software in order to compute the permeability in a sheared unit cell. To validate the results, we compare the computations with analytical formulas from Lai and Young [34]. They present formulas for the direction of the principal axis of the sheared textile β as function of the shear angle θ, and also for the rate of anisotropy ($\tilde{\alpha} = \frac{K_{xx}}{K_{yy}}$) as function of θ

$$\beta = \frac{1}{2}\tan^{-1}\left(\frac{m\sin(2\theta)}{1-\alpha-2m\sin^2(\theta)}\right),$$

$$\tilde{\alpha} = \frac{\sin^2(\beta-\theta)-\alpha\cos^2(\beta)}{\alpha\sin^2(\beta)-\cos^2(\beta-\theta)}. \qquad (6)$$

Here, α is the anisotropy of the undeformed textile, and m is a parameter which depends on the barrier effect on the flow of the yarns in the warp direction. These formulas are based on a mathematical description of the elliptical flow front, the assumptions that the flow rates in warp and weft direction of the deformed textile are kept at the same ratio, and that for the deformed fabric the tangent of the flow front in the warp direction is parallel to the weft direction.

For different shear angles θ, Fig. 5 compares the numerical computed principal direction with the direction computed using the formula of Lai and Young. Additionally, the figure shows the numerical and analytical permeability ratios. We can conclude that the theoretical results agree well with the numerical values.
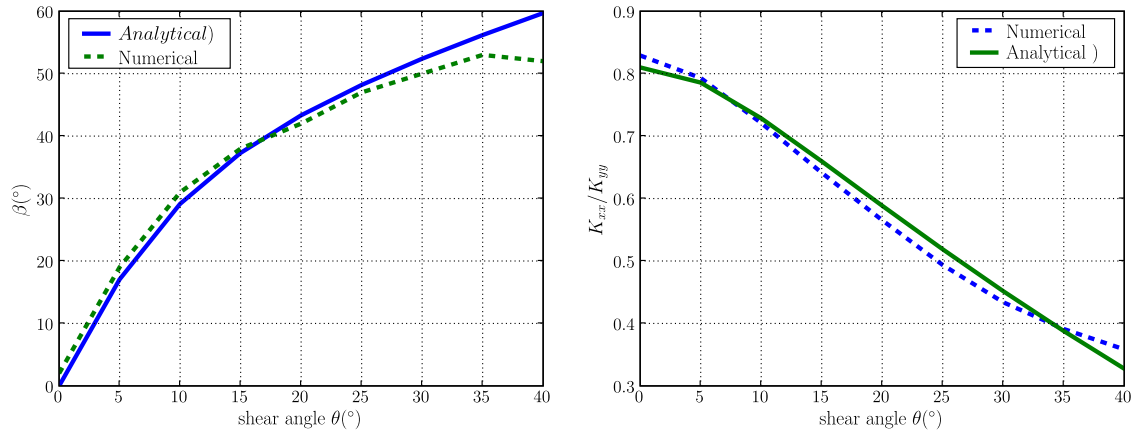
Fig. 5. As function of the shear angle: the direction of the principal axis (left) and the anisotropy (right).
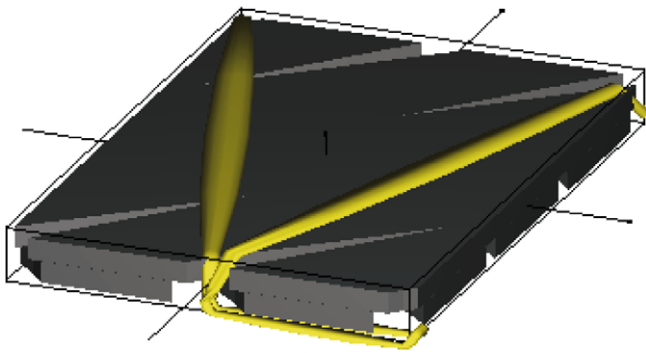

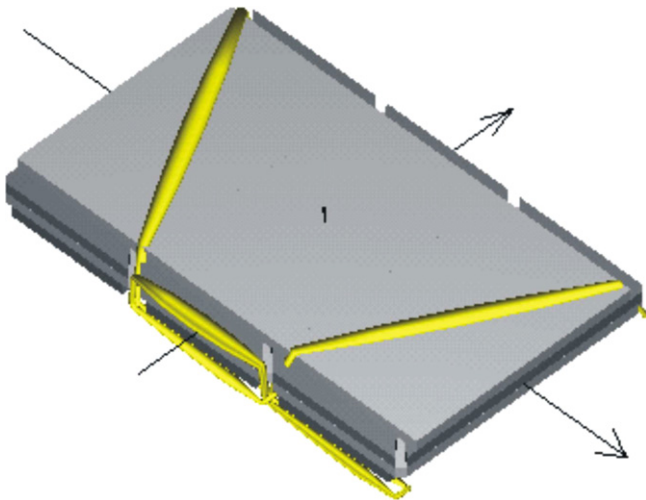**Fig. 6.** Bi-axial non-crimp fabric.
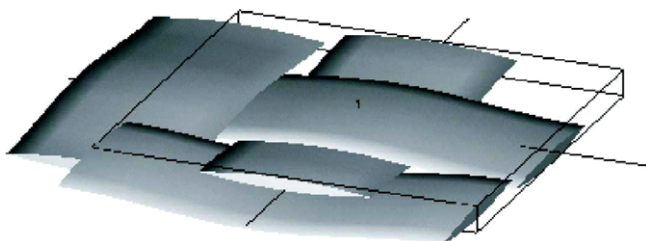

Fig. 7. Quadri-axial non-crimp fabric.

Fig. 8. The plain woven fabric.

5.4. Computation time

As mentioned in Section 3, the Navier–Stokes solver uses time stepping to reach the steady state solution in which we are interested. This time stepping procedure can be performed semi-implicitly or explicitly. If semi-implicit time stepping is used, the stability criterion is less restrictive and time steps can be enlarged which results in faster solution times (Table 5). The Stokes solver computes the steady state solution directly, and is substantially faster than the time stepping methods. For a fine grid, $\Delta x = 0.02$ mm, the solver only needs approximately 1 min.

6. Conclusions

In this paper, a general approach for the computation of the permeability of textiles was presented. Solving the Stokes equations with a finite difference discretisation on a regular grid has the advantage that the solver can be used for any kind of textile structure without meshing problems. Although methods designed for specific textiles may lead to a faster solution, they only work for that specific structure and have to be redeveloped for new textiles. Moreover, fast and reliable solvers for PDEs are used in our permeability simulations.
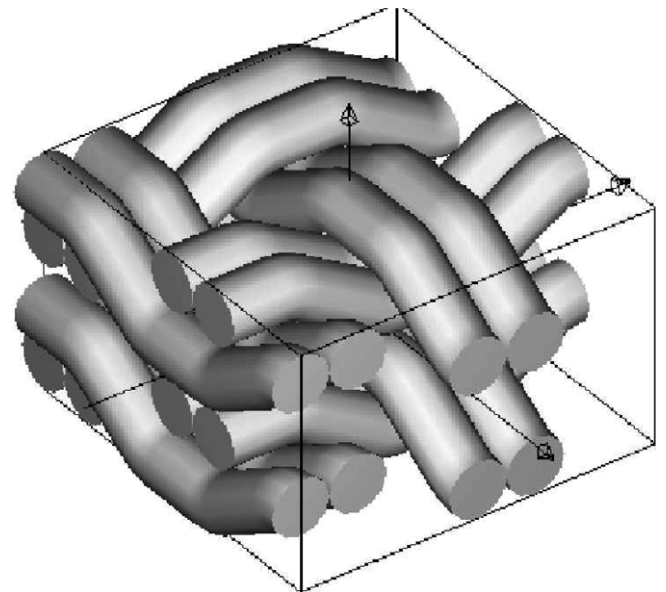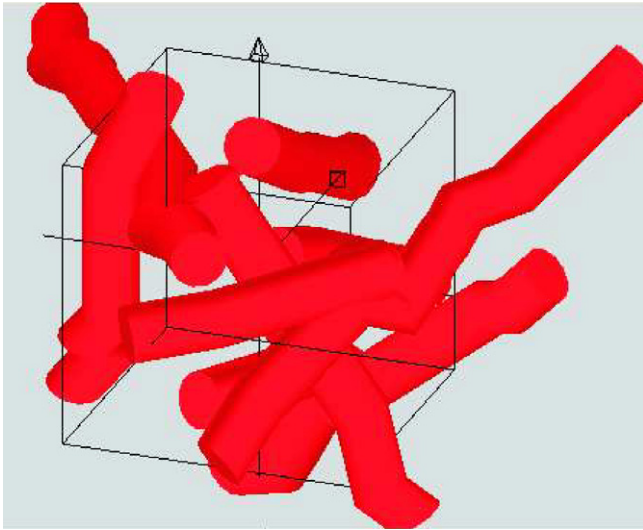

Fig. 9. The mono-filament fabric.

Fig. 10. Unit cell of a random mat.

Table 5
Permeability values and computation time for a single layer model with XYZ periodic boundary conditions of the MFF

Δx (mm)	K_{xx} (mm^2)	Comp. time NaSt3D	Comp. time stokes
0.02	3.3 E−04	16 min 00 s	00 min 46 s
0.03	3.4 E−04	03 min 40 s	00 min 26 s
0.04	4.3 E−04	01 min 11 s	00 min 05 s

We have presented experimental validation for different textiles: non-crimp fabrics, woven fabrics and a random mat. Computations on a single layer model with periodic boundary conditions result in a small over-estimation of the experimental value, as nesting is neglected. Therefore, multi-layered models are to be used in the simulations, and wall conditions should be imposed. For textiles with a high volume fraction, intra-yarn flow has an important influence on the permeability value. The micro flow is accounted for by solving the Brinkman equations.

Not only nesting, boundary conditions and intra-yarn flow influence the permeability, also the shear of the specimen plays an important role. Our method is able to model shear and compute the permeability of the sheared models.

Acknowledgements

References

[1] Available from: http://www.esi-group.com.
[2] Simacek P, Sozer E, Advani S. User manual for DRAPE 1.1 and LIMS 4.0 (Liquid Injection Molding Simulation), Technical Report 98-01, University of Delaware, Center for Composite Materials; 1998.
[3] Gebart B. Permeability of unidirectional reinforcements for RTM. J Compos Mater 1992;26(8):1100–33.
[4] Berdichevski A, Cai Z. Preform permeability predictions by selfconsistent method and finite element simulation. Polym Compos 1993;14(2):132–43.
[5] Phelan F, Wise G. Analysis of transverse flow in aligned fibrous porous media. Compos part A 1996;27A:25–34.
[6] Verleye B, Klitz M, Croce R, Griebel M, Lomov S, Roose D, et al. Predicting the permeability of textile reinforcements via a hybrid Navier–Stokes/Brinkman solver. In: Proceedings of the 8th international conference on flow processes in composite materials, Douai, France; 2006.
[7] Wong C, Long A, Sherburna M, Robitaille F, Harrison P, Rudd C. Comparisons of novel and efficient approaches for permeability prediction based on the fabric architecture. Compos Part A 2006;37(6):847–57.
[8] Verleye B, Lomov S, Long A, Wong C, Roose D. Permeability of textile reinforcements: efficient prediction and validation. In: Kageyama K, Ishikawa T, Takeda N, Hojo M, Sugimoto S, Ogasawara T, editors. Proceedings of the 6th international conference on composite materials, Japan Society for Composite Materials; 2007, p. 220–1.
[9] Belov E, Lomov S, Verpoest I, Peeters T, Roose D. Modelling of permeability of textile reinforcements: lattice Boltzmann method. Compos Sci Technol 2004;64:1069–80.
[10] Laine B, Hivet G, Boisse P, Boust F, Lomov S, Badel P. Permeability of the woven fabrics. In: Binetruy C. editor. Proceedings of the 8th international conference on flow processes in composite materials, Ecole des Mines de Douai, France; 2006, p. 39–46.
[11] Takano N, Zako M, Okazaki T, Terada K. Microstructure-based evaluation of the influence of woven architecture on permeability by asymptotic homogenisation theory. Compos Sci Technol 2002;62:1347–56.
[12] Robitaille F, Long A, Sherburn M, Wong C, Rudd C. Predictive modelling of processing and performance properties of textile composite unit cells: current status and perspectives. In: Proceedings ECCM-11, 2004, cd-edition.
[13] Delerue J, Lomov S, Parnas R, Verpoest I, Wevers M. Pore network modelling of permeability for textile reinforcements. Polym Compos 2003;24(3):344–57.
[14] Siclen CV. Walker diffusion method for calculation of transport properties of finite composite systems. Phys Rev E 2002;65:1–6.
[15] Verpoest I, Lomov S. Virtual textile composites software Wisetex: integration with micro-mechanical, permeability and structural analysis. Compos Sci Technol 2005;65(15–16):2563–74.
[16] Lomov S, Mikolanda T, Kosek M, Verpoest I. Model of internal geometry of textile composite reinforcements: data structure and virtual reality implementation. J Textile Inst 2007;98(1):1–13.
[17] Lomov S, Ivanov D, Verpoest I, Zako M, Kurashiki T, Nakai H, et al. Meso-FE modelling of textile composites: road map, data flow and algorithms. Compos Sci Technol 2007;67:1870–91.
[18] Gresho P, Sani RL. On pressure boundary conditions for the incompressible Navier–Stokes equations. Int J Numer Methods Fluids 1987;7:1111–45.
[19] Verleye B, Klitz M, Croce R, Roose D, Lomov S, Verpoest I. Computation of permeability of textile with experimental validation for monofilament and non-crimp fabrics. Comput Textiles, vol. 55. Berlin: Springer; 2007.
[20] Brinkman H. On the permeability of media consisting of closely packed porous particles. Appl Sci Res 2001;1(1):81–6.
[21] Angot P. Analysis of singular perturbations on the Brinkman problem for fictious domain models of viscous flow. Math Methods Appl Sci 1999;22:1395–412.
[22] Available from: http://wissrech.iam.uni-bonn.de/research/projects/NaSt3DGP.
[23] Griebel M, Dornseifer T, Neunhoeffer T. Numerical simulation in fluid dynamics, a practical introduction. Philadelphia: SIAM; 1998.
[24] Balay S, Buschelman K, Gropp WD, Kaushik D, Knepley MC, McInnes LC, et al. Available from: http://www.mcs.anl.gov/petsc.
[25] Elman H, Howle V, Shadid J, Silverster D, Tuminaro R. Least squares preconditioners for stabilized discretizations of the Navier-Stokes equations. SIAM J Sci Comput 2006;27:1651–68.
[26] Elman HC, Silvester DJ, Wathen AJ. Finite elements and fast iterative solvers. Oxford: Oxford University Press; 2005.
[27] Hoes K. Development of a new sensor-based setup for experimental permeability identification of fibrous media, Ph.D. thesis, Vrije Universiteit Brussel; 2003.
[28] Hoes K, Dinescu D, Sol H, Vanheule M, Parnas R, Luo Y, et al. New set-up for measurement of permeability properties of fibrous reinforcements for rtm. Compos Part A 2002;33(7):959–69.
[29] Morren G. Gu J. Sol H, Verleye B, Lomov S. Permeability identification of a reference specimen using an inverse method, in: SEM Annual Conference and Exposition; 2007, cd-edition, p. 1–8.
[30] Morren G, Gu J, Sol H, Verleye B, Lomov S. Stereolithography specimen to calibrate permeability measurements for RTM flow simulations. Adv Comp Lett 2006;15(4):119–25.
[31] Nordlund M, Lundstrom TS. Numerical study of the local permeability of non-crimp fabrics. J Compos Mater 2005;39(10):929–47.
[32] Lomov S, Verpoest I, Peeters T, Roose D, Zako M. Nesting in textile laminates: geometrical modelling of the laminate. Compos Sci Technol 2002;63(7):993–1007.
[33] Lomov S, Verpoest I. Model of shear of woven fabric and parametric description of shear resistance of glass woven reinforcements. Compos Sci Technol 2006;66(7-8):919–33.
[34] Lai C, Young W. Model resin permeation of fiber reinforcements after shear deformation. Polym Compos 1997;18(5):642–8.